Available online at www.sciencedirect.com
ScienceDirect
Journal of Chromatography A, 1161 (2007) 269–274
JOURNAL OF CHROMATOGRAPHY A
www.elsevier.com/locate/chroma

Separation of dialkyl sulfides by metallomesogenic stationary phases for complexation gas chromatography

Jian-Lian Chen [a,*], Chuen-Ying Liu [b,**]

[a] *Department of Occupational Safety and Health, Chung Shan Medical University, Taichung, Taiwan*
[b] *Department of Chemistry, National Taiwan University, Taipei, Taiwan*

Received 10 April 2007; received in revised form 22 May 2007; accepted 29 May 2007
Available online 2 June 2007

Abstract

A copper mesogenic side-chain polymer (P-$C_{15}CuC_{18}$) was cross-linked onto the capillary wall as a stationary film for gas chromatography (GC) separation of alkylsulfides. These organic sulfides are of interest for their large health impact because of their wide range of volatilities and high reactivities toward metals. Different GC parameters for optimal separation efficiency are discussed for use with a mesogenic polymer column along with flame photometric detection (FPD). Both the carrier gas flow-rate and column temperature were studied to determine the relationship of plate height to the chemical structure of the solutes, as well as to determine the morphology of the mesogenic polymer. Van 't Hoff plots show phase transitions of the stationary mesophase as the column temperature was varied. The results reveal that the separation mechanism might be based on ligand exchange and polarity interaction between the analytes and the stationary phase, with the vapor pressure of the analytes also being important. The former interaction dominates in the lamellar crystalline phase and the latter interaction dominates in the hexagonal columnar-discotic phase. With high reproducibility for retention time (RSD $\leq$ 0.37%) and for peak area (RSD $\leq$ 5.16%), the GC–FPD system produced linear calibration graphs ($r \geq 0.9918$) for the determination of 13 sulfides with a detection limit below 2.5 ng.

Keywords: Metallomesogen; Stationary phase; Complexation GC; Dialkyl sulfide

1. Introduction

Metallomesogens or metal-containing liquid crystals have gained great interest during recent years for their unique properties derived from the presence of metal ions within anisotropic phases [1–4]. The presence of one or more metals offers many exciting possibilities, because the coordination of metal ions may lead to properties not found readily in organic mesogens. A search for highly selective stationary phases is an important trend of chromatography development. Recently, Witkiewicz et al. [3] reviewed the current state of the art in the use of liquid crystalline including metallomesogenic stationary phases for gas chromatography (GC). Separations with the metallomesogenic stationary phase can be considered as one example of the more popular complexation chromatography [5–7].

Among thermotropic liquid crystals, both rod-like (calamitic) and disk-like (discotic) metallomesogens have been employed as the stationary phases for the separation of close-boiling isomers, which are very difficult or impossible to separate on classical stationary phases [8–13]. Both shape recognition and ligand exchange were found to be the main separation mechanism in these processes. Columnar stationary mesophases, which could be formed from the stacking of discotic mesogens, is adapted to recognize flat-round-shaped analytes. Copper stearate, the disk-like dinuclear tetraalkanoate, is one of the examples. A side chain polymer with copper carboxylato discotic units in stacks has been prepared for the satisfactory separation of phenols [11] and phthalates [12].

Sulfur compounds are present to some extent in all fuels. Both volatile sulfur compounds (VSCs) and lower-volatility sulfur compounds are found in industrial activities [14–16]. Dialkyl sulfides are important compounds of wide interest to scientists from viewpoint of analytical, environmental, synthetic, medicine and material science [17–19]. The detection of sulfide has gained significant importance within the analytical community as a consequence of toxicological research and

* Corresponding author. Tel.: +886 4 24730022; fax: +886 4 23248194.
** Corresponding author. Tel.: +886 2 33661645; fax: +886 2 23638543.
E-mail addresses: cjl@csmu.edu.tw (J.-L. Chen), cyliu@ntu.edu.tw (C.-Y. Liu).

0021-9673/$ – see front matter © 2007 Elsevier B.V. All rights reserved.
doi:10.1016/j.chroma.2007.05.084

the risks associated with occupational exposure [20,21]. The VSCs, such as dialkyl sulfides in a variety of matrices have been analyzed using the headspace solid-phase microextraction coupled with GC [22–24]. A two-dimensional GC method was necessary for the separation of sulfur compounds in crude oil [25].

A universal column with efficient modes of separation for sulfur analytes having a variety of physicochemical properties is therefore expected to replace the special support of a GC × GC software package and an interface modulator. A metallomesogenic stationary phase would be a candidate for this purpose. Both rod-like and disk-like sulfur-ligand metallomesogens coated on Chromosorb W as packed columns have been employed for the GC separation of dialkyl sulfides [8,13]. In this study, 13 alkyl sulfides (C_2–C_{16}) were mixed as a sample with a broad span of volatilities, to evaluate the separation efficiency of a capillary column coated with discotic copper-mesogenic polymer along with the flame photometric detection (FPD) system.

2. Experimental

2.1. Apparatus

The gas chromatograph used for column evaluation was a Shimadzu model 17A equipped with a capillary column split-injection system and an FPD system. The major components of the FPD system were a 394 nm filter, a base block, and a head block. The base block is sited between the capillary adaptor and the flame nozzle. There is a quartz tube in the base block. It should be at least 30 °C higher than the column thermostat to prevent the analytes from being condensed in the tube. The head block is sited above the flame nozzle, and heated between 100 and 200 °C to prevent flame ashes from being condensed in a quartz cylinder of the block. However, if the heating is more than 200 °C, it would damage the detector components, such as the filter and the photomultiplier tube. In the following experiments, the base block and the head block were set at 230 °C and 150 °C, respectively. Chromatograms were plotted on a Shimadzu CR-6A Chromatopac integrator.

2.2. Chemicals and materials

The 13 organic sulfides used for this study are: dimethyl sulfide (b.p. 37 °C), allyl methyl sulfide (91–93 °C), diethyl sulfide (92 °C), *tert*-butyl methyl sulfide (102 °C), diisopropyl sulfide (121 °C), diallyl sulfide (138 °C), di-*n*-propyl sulfide (142 °C), pentamethylene sulfide (142 °C), di-*tert*-butyl sulfide (147–151 °C), di-*sec*-butyl sulfide (165 °C), di-*n*-butyl sulfide (188 °C), di-*n*-hexyl sulfide (230 °C), and di-*n*-octyl sulfide (310 °C). The sulfur compounds were obtained either from Aldrich (Milwaukee, WI, USA) or TCI (Tokyo, Japan). The stock solutions of these analytes (4×10^6 μg mL^{-1}) were prepared in *n*-hexane and kept at 4 °C.

Deactivated fused silica capillaries (20 m × 0.25 mm I.D., Restek, Bellefonte, PA, USA) were first rinsed with methanol and dichloromethane to remove impurities from the capillary wall surface before the dynamic coating of P-$C_{15}CuC_{18}$, a discotic copper complex-containing siloxane polymer (Fig. 1). The synthesis and the capillary wall coating of P-$C_{15}CuC_{18}$ with a cross-linking network were as described [11].

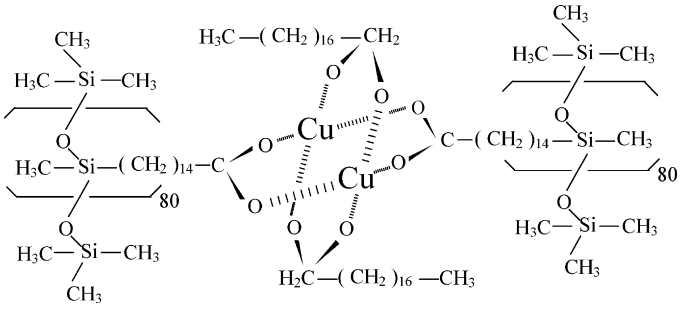

Fig. 1. Structure of P-$C_{15}CuC_{18}$, the mesogenic side-chain polymer used in column coating.

2.3. GC analysis

Injector temperature set at 250 °C was selected using a test range of 220–270 °C, and by monitoring the FPD signal intensity of di-*n*-propyl sulfide, which was chosen for its intermediate boiling point among the 13 sulfides. To evaluate the effect of carrier gas velocity and column temperature on retention beyond the effects of natural thermal diffusibility, five sulfides (diethyl, *tert*-butyl methyl, diisopropyl, diallyl, and di-*tert*-butyl sulfide) were regarded as group I and displayed relatively lower vapor pressures than those of group II (di-*n*-propyl, di-*sec*-butyl, di-*n*-butyl, and pentamethylene sulfide). The two sulfide groups were analyzed separately, along with a sample containing all the sulfide compounds. A portion (1 μL) of each sample was injected into the GC–FPD system. High-purity nitrogen was used as the carrier gas. A split ratio of 30:1, and an injector purge flow of 3 mL/min were maintained throughout the experiments.

By varying the carrier gas inlet pressure from 5 to 40 kPa, the theoretical plate height could be obtained from the peak information under a controlled column temperature of 40 °C for group I, and 70 °C for group II. In addition, the column linear velocity was calculated from the column length and gas hold-up time, which was determined by the injection of *n*-hexane to the same conditioned GC module with flame ionization detection (FID).

3. Results and discussion

3.1. Effect of carrier gas flow rate

3.1.1. Group I sulfides

The group I sulfides with lower boiling point, were influenced strongly by the inlet N_2 pressure, which for 5, 10 and 15 kPa yielded 0.1 mL/min, 0.2 mL/min and 0.3 mL/min capillary flow-rates, or 2.05 cm/s, 3.27 cm/s and 4.65 cm/s linear velocities, respectively. The results indicated that higher inlet pressure gives faster elution rate. The elution rate decreased

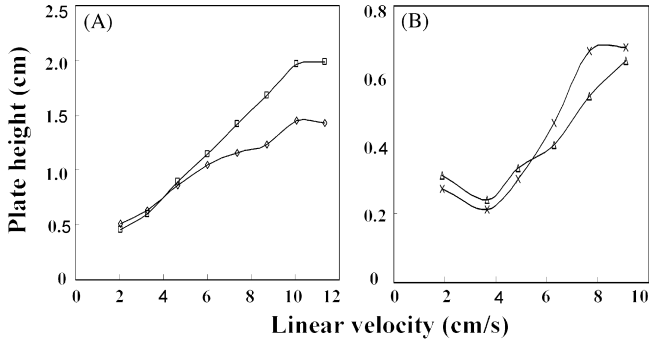

Fig. 2. Effect of carrier gas flow-rate on plate height. Capillary column, 20 m × 250 μm I.D.; wall-coated with copper carboxylate complex, P-$C_{15}CuC_{18}$; sample concentration, 30 μg/mL except di-*tert*-butyl sulfide 95 μg/mL, and diallyl sulfide 95 μg/mL; injection volume, 1 μL; split ratio: 30; injector temperature, 250 °C; oven temperature, 40 °C; FPD base and head block temperature, 230 and 150 °C. (A) di-*tert*-butyl sulfide (◊) and diallyl sulfide (□); (B) di-*n*-propyl sulfide (△) and di-*sec*-butyl sulfide (×).

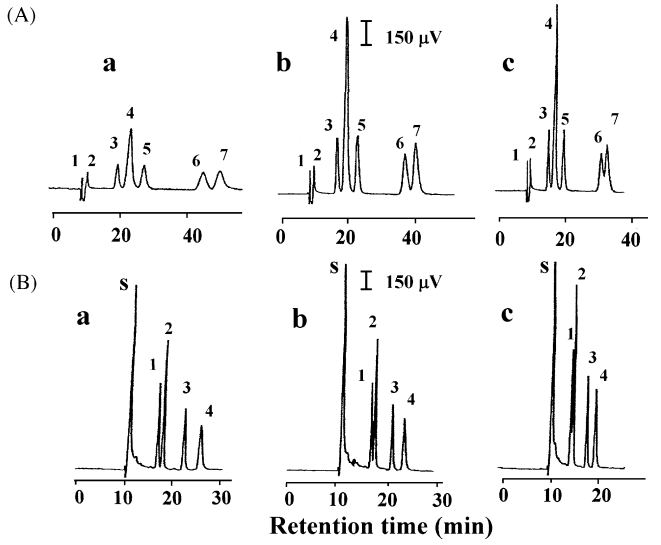

Fig. 3. The separation of organic sulfides under isothermal conditions. Capillary column, 20 m × 250 μm I.D.; wall-coated with copper carboxylate complex, P-$C_{15}CuC_{18}$; sample concentration, 30 μg/mL except diisopropyl sulfide 63 μg/mL, di-*tert*-butyl sulfide 95 μg/mL, and diallyl sulfide 95 μg/mL; injection volume, 1 μL; split ratio: 30; injector temperature, 250 °C; oven temperature, 40 °C; FPD base and head block temperature, 230 and 150 °C; N_2 inlet pressure, 10 kPa. Column temperature: (A) a = 35 °C, b = 40 °C, c = 45 °C; (B) a = 70 °C, b = 75 °C, c = 80 °C. Peak identification: (A) 1, dimethyl sulfide; 2, allyl methyl sulfide; 3, *tert*-butyl methyl sulfide; 4, diethyl sulfide; 5, diisopropyl sulfide; 6, di-*tert*-butyl sulfide; 7, diallyl sulfide. (B) s = system peak; 1, di-*n*-propyl sulfide; 2, di-*sec*-butyl sulfide; 3, pentamethylene sulfide; 4, di-*n*-butyl sulfide.

as the following order: allyl methyl sulfide > *tert*-butyl methyl sulfide > diethyl sulfide > diisopropyl sulfide > di-*tert*-butyl sulfide > diallyl sulfide.

The effect of flow-rate on the plate height for di-*tert*-butyl sulfide and diallyl sulfide, which are representative of the other sulfides, was studied. According to the close match of the two van Deemter curves (Fig. 2A), it is speculated that the longitudinal diffusion coefficient *B* for diallyl sulfide might be lower than that of di-*tert*-butyl sulfide, but the mass-transfer coefficient *C* value is higher. This suggests a lower diffusibility and a slower desorption rate for diallyl sulfide than that for di-*tert*-butyl sulfide. A strong coordination of the allyl group, which bears a double-bond structure, to the copper acceptor on the stationary phase could be considered the reason for the slower mass-transfer of diallyl sulfide. Even though the boiling point of diallyl sulfide is lower than that of di-*tert*-butyl sulfide, the latter was eluted earlier. This is reasonable, as it has been shown that the Lewis acid–base interaction prevailed in the lamellar crystalline stationary phase with more "visible" or approachable copper atoms [26]. This result therefore follows a normal pattern of complexation GC.

3.1.2. Group II sulfides

For group II analytes, the behaviors of the inlet pressure-influenced retentions are similar to those for group I analytes. The retention affinity increased as the following order: di-*n*-propyl sulfide > di-*sec*-butyl sulfide > pentamethylene sulfide > di-*n*-butyl sulfide. The effects of flow-rate on plate height indicated that di-*sec*-butyl sulfide demonstrated a more impeded mass-transfer between the nitrogen mobile phase and the discotic lamellar stationary phase than di-*n*-propyl sulfide (Fig. 2B). In fact, di-*sec*-butyl sulfide with higher boiling point was eluted after di-*n*-propyl sulfide. It is not easy to reach any conclusion for the results shown in Fig. 2B on the basis of the structure difference in alkyl groups.

Eventually, the inlet pressure of 10 kPa was set for both sulfide groups.

3.2. Effect of column temperature

Column temperature affects both the vaporization of the analyte and the molecular arrangement of the metallomesogenic stationary phase. The group I and group II sulfides were studied at 35–70 °C and 60–95 °C respectively, and showed signs of retention in the two phase ranges: crystalline-to-discotic lamellar (D_L) and D_L-to-hexagonal columnar-discotic (D_{ho}). The chromatograms shown in Fig. 3A and B demonstrated that the behavior of solute partitioning into stationary phases, specifically regarding the mesomorphic structure, was effectively controlled by oven temperature. This control was seen with temperature changes of only 5 °C. The first highest peak for group analytes in Fig. 3B was considered as a system peak after identification for each analyte. Moreover, the system peak might be assumed coming from the incorporation of the more volatile group I sulfides.

By plotting plate height versus column temperature, a non-linear relationship was obtained as shown in Fig. 4. For the more volatile compounds of group I, i.e. *tert*-butyl methyl sulfide and diethyl sulfide, higher column temperatures resulted in smaller plate heights, as seen in Fig. 4A. These molecules were vaporized and escaped with higher mobility from the hot GC injector; soon afterwards the jet velocity was increased by the higher column temperature. Here, the zone broadening from the longitudinal diffusion was largely suppressed and apparently dominated the separation efficiency. For the less volatile probes of group II, i.e. di-*n*-propyl sulfide and di-*sec*-butyl sulfide, the

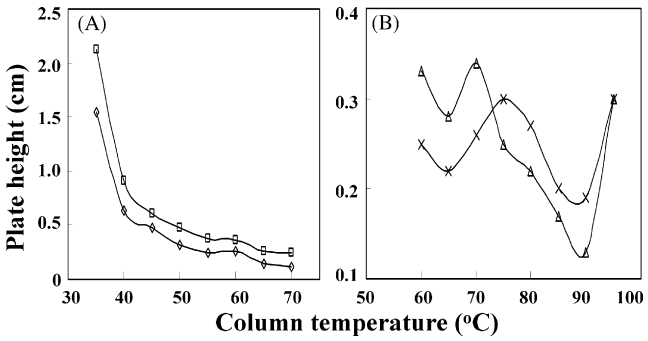

Fig. 4. Effect of column temperature on plate height. GC–FPD conditions as in Fig. 3. (A) *tert*-butyl methylsulfide (◊) and diethylsulfide (□); (B) di-*n*-propylsulfide (△) and di-*sec*-butylsulfide (×).

trend lines in Fig. 4B indicate that the mass-transfer equilibrium would be greatly involved in the separation efficiency of some stationary mesophases. Each line has two inflection points, and therefore two phases should exist in the temperature range of 60–95 °C. The temperature range between the inflection points of the curved lines might correspond to the transition temperature of the coppermesogenic polymer film anchored to the capillary wall. Here, 70–80 °C corresponding to the transition of D_L to D_{ho}, was lower than that in the bulk liquid (95 °C), which was determined by differential scanning calorimetry (DSC) [11]. This inconsistency could be due to a certain amount of "locked" mobility of the cross-linked polymer film and/or a different heating rate compared with that of the DSC experiments.

The van't Hoff plot in Fig. 5 shows the dependence of solute partitioning into the mesogenic film on reciprocal absolute column temperature. With the consideration of the solute–solvent diffusivity, there are two mesogenic phases, D_L and D_{ho} shown in Fig. 5B, while crystalline and D_L phases are shown in Fig. 5A. Since the compatibility of all the substituted sulfides with the heat-sensitive stationary phase could not be equivalent, a variation of the solute solubility between the two polymeric phases resulted in the discontinuous linearity of the lines in Fig. 5, which suggests a distinct phase transition.

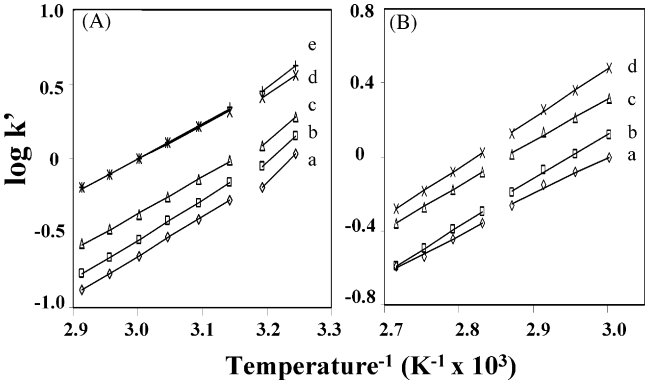

Fig. 5. Van't Hoff plots of organic sulfides. GC-FPD conditions as in Fig. 3. (A) a = *tert*-butyl methyl sulfide, b = diethyl sulfide, c = diisopropyl sulfide, d = di-*tert*-butyl sulfide, e = diallyl sulfide; (B) a = di-*n*-propyl sulfide, b = di-*sec*-butyl sulfide, c = pentamethylene sulfide, d = di-*n*-butyl sulfide.

3.3. Optimum separation conditions and linear calibration range

It is not easy to separate all of the sulfide targets isothermally within a reasonable time, as their boiling points range from 37 to 310 °C. However, according to the isothermal results shown in Fig. 3A (b), the sulfides with lower boiling points could be well separated within 43 min when the column temperature was maintained at 40 °C. We supposed that the remaining sulfides would be eluted subsequently with an appropriate rate of temperature increase. The programmed-temperature separation with rising rates of 50, 60 and 70 °C min^{-1} was carried out from 40 °C (hold 43 min) then to 170 °C. The most satisfactory chromatogram was achieved at a rate of 60 °C min^{-1} (Fig. 6). Under optimized conditions, the reproducibility for the determination of sulfide standards assessed from ten measurements is given in Table 1. The RSD for retention time was less than 0.37%, and

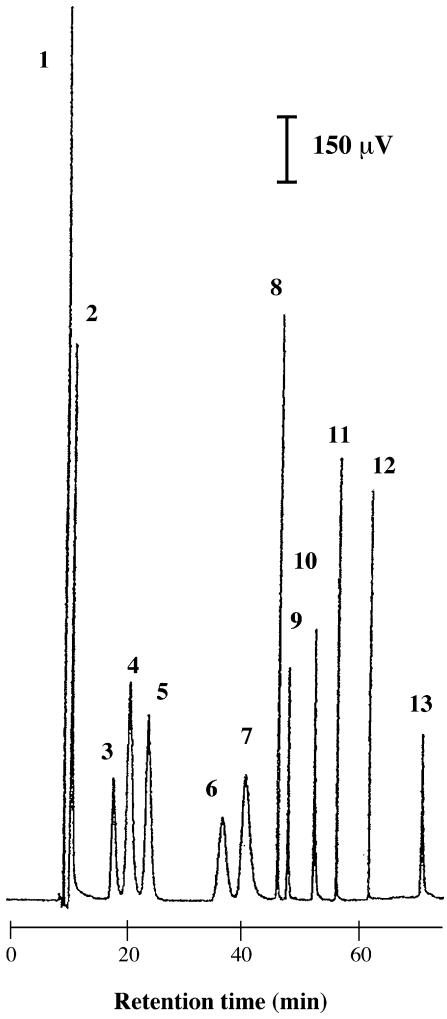

Fig. 6. Programmed-temperature separation of organic sulfides. GC–FPD conditions as in Fig. 3, except that the column temperature was 40 °C (43 min) to 170 °C at 60 °C min^{-1}. Peak identification: 1, dimethyl sulfide; 2, allyl methyl sulfide; 3, *tert*-butyl methyl sulfide; 4, diethyl sulfide; 5, diisopropyl sulfide; 6, di-*tert*-butyl sulfide; 7, diallyl sulfide; 8, di-*n*-propyl sulfide; 9, di-*sec*-butyl sulfide; 10, pentamethylene sulfide; 11, di-*n*-butyl sulfide; 12, di-*n*-hexyl sulfide; 13, di-*n*-octyl sulfide.

Table 1
Summary for the determination of organic sulfides in the GC–FPD system[a]

Compound	Regression equation[b] (y: peak area, μV s; x: concentration, μg mL^{-1})	Correlation coefficient	Detection limit[c] (ng)	Retention time RSD[d] (%)	Peak area RSD[d] (%)
Dimethylsulfide	Log y = 2.1156 log x + 2.1016	0.9992	0.7	0.37	5.16
Allyl methyl sulfide	Log y = 2.0425 log x + 1.3233	0.9923	2.4	0.33	4.87
t-Butyl methyl sulfide	Log y = 2.0413 log x + 1.2580	0.9976	2.5	0.35	3.20
Diethyl sulfide	Log y = 1.9156 log x + 2.0632	0.9933	1.7	0.25	1.59
Diisopropyl sulfide	Log y = 2.2543 log x + 1.5877	0.9918	1.6	0.19	1.79
Di-*tert*-butylsulfide	Log y = 2.0883 log x + 1.5610	0.9929	2.2	0.32	1.92
Diallyl sulfide	Log y = 2.4199 log x + 1.1203	0.9953	2.0	0.20	3.63
Di-*n*-propyl sulfide	Log y = 2.0042 log x + 2.3746	0.9974	0.5	0.20	4.56
Di-*sec*-butyl sulfide	Log y = 1.9672 log x + 2.0342	0.9953	1.1	0.02	1.44
Pentamethylene sulfide	Log y = 2.4160 log x + 1.3937	0.9982	1.1	0.03	1.35
Di-*n*-butyl sulfide	Log y = 2.2930 log x + 1.8586	0.9988	0.7	0.04	1.46
Di-*n*-hexyl sulfide	Log y = 2.0095 log x + 2.2527	0.9957	0.7	0.08	1.16
Di-*n*-octyl sulfide	Log y = 2.1887 log x + 1.5980	0.9920	1.7	0.18	2.63

[a] Conditions as in Fig. 6.
[b] Sample concentration range from 2.0 to 126 μg mL^{-1}.
[c] Defined by three times standard deviation for the peaks of seven measurements with the least amount that could be detected.
[d] Relative standard deviation assessed from 10 measurements.

the RSD for peak area was less than 5.16%. Most of the high RSD values came from the highly volatile analytes.

The relationship between the FPD response and the concentration of the injected sample was studied. The calibration equations of log (peak area, μV s) against log (concentration, μg mL^{-1}) for each analyte are shown in Table 1. The linear range is from 2.0 to 126 μg mL^{-1}. The correlation coefficients are greater than 0.9918. The detection limit, defined as three times the standard deviation for the peaks of seven continuous measurements of the least detectable analyte amount, was less than 2.5 ng.

3.4. Separation mechanism

The factors responsible for the elution order found with the above isothermal conditions were based on the interaction between the gaseous sulfides and the thermotropic separation bed, each with their own distinctive physicochemical properties. An earlier multi-linear model described this interaction successfully and quantitatively [26]. That report concluded that the Lewis acid–base interaction, namely complex formation between analytes and the stationary phase prevails in the lamellar crystalline phase, and that the polarity interaction dominates in the D_{ho} phase. In addition, the D_L phase with moderate molecular ordering will probably experience all three interactions, including dispersion. The following is a qualitative statement about the mechanism involved in a mixed separation mode, and agrees well with the earlier report.

3.4.1. Ligand exchange

The chromatograms in Fig. 6 show that, for the most part, the GC elution order followed that of the boiling points of the alkylsulfides. However, in spite of the importance of volatility, which may contribute a great thermostatic effect on the gaseous population and a kinetic effect regarding the concomitant action of partitioning in the column, other forces indeed played prominent roles in the elution order.

The sulfur atom with unpaired electrons in the analyte could associate with the stationary phase, which has an empty orbital on the central metal atom. In theory, the presence of longer alkyl groups on the analyte would exhibit a higher boiling point, greater electron density around the sulfur atom and, consequently, a stronger coordination with the copper atoms. In fact, the retention time increased in the order: $n = 1 < 2 < 3 < 4 < 6 < 8$, where n is n-alkyl number. Nevertheless, this order is not very convincing evidence to prove that ligand exchange is involved; this supposed mechanism might be disregarded because of the greater influence of solute volatility. The only clues that could be found were *tert*-butyl methyl sulfide (b.p. 102 °C) being eluted before diethyl sulfide (92 °C), and di-*tert*-butyl sulfide (147–151 °C) eluted before diallyl sulfide (138 °C). The bulky *tert*-butyl group resulted in less affinity for the coordination with the mesogenic phase, thus being less retained in the column. Furthermore, those with π-donating electrons in the alkyl chain, e.g. allyl groups, could intrinsically contribute to greater retention.

3.4.2. Polarity interaction

The mesogenic phase has low polarity. Although the dipole–dipole interaction does not occur for solutes with symmetrical molecular structure, the induced dipole–dipole interaction does take place with sulfides, for which polarizability contributions from n- and π-electrons could be actuated by the slightly polar mesophase. The induced interaction would be enhanced if the solute molecular configuration is spatially compatible with that of the mesogen molecule. Hence, di-*sec*-butyl sulfide (b.p. 165 °C) was eluted before pentamethylene sulfide (142 °C), because the latter sulfide, with its disk-like shape, was similar in shape to the columnar polymer in the D_{ho} state.

4. Conclusions

Upon optimization of the GC operation parameters, the retention behaviors give useful information on the interactions between solute and liquid crystalline molecules. They reveal

how the interactions corresponded to the mesomorphic textures and physicochemical properties of the solutes. This information was not only crucial to the chromatographic selectivity of the analytes, but also helpful in the logical design of a suitable mesophase for more specific separations.

The separation mechanism of mesogenic stationary phases is mostly connected with the structure differentiation of the chromatographed substances [27]. In this work, the mesogenic phases seen with changes in column temperature were correlated closely to the solute-partitioning interactions and separation efficiency. Specific mechanism in a mixed separation mode, including ligand exchange and shape recognition, was revealed from the van Deemter plots and the chromatographic elution order. The established GC–FPD module for the separation of 13 alkyl sulfides is another example of the use of a dinuclear copper-mesogenic polymer [11]. By comparison with the results using a sulfur-ligand mesogen [8,13], the discotic oxygen-ligand mesogen provides more well-resolved peaks. This GC-FPD system with high selectivity, high reproducibility and a low detection limit would be applicable to a direct analysis of complex matrix sulfur-containing samples.

Acknowledgement

The authors thank the National Science Council of Taiwan for the financial support.

References

[1] L. Oriol, J.L. Serrano, Angew. Chem. Int. Ed. Engl. 44 (2005) 6618.
[2] B. Donnio, D. Guillon, R. Deschenaux, in: J.A. McCleverty, T.J. Meyer (Eds.), From the Molecular to the Nanoscale: Synthesis, Structure, and Properties (Comprehensive Coordination Chemistry II, vol. 7), Elsevier, Amsterdam, Oxford, 2004, p. 357.
[3] Z. Witkiewicz, J. Oszczudłowski, M. Repelewicz, J. Chromatogr. A 1062 (2005) 155.
[4] J.L. Serrano (Ed.), Metallomesogens—Synthesis, Properties, and Applications, VCH, Weinheim, 1996.
[5] D. Cagniant (Ed.), Complexation Chromatography, Marcel Dekker, New York, 1992.
[6] V. Schurig, in: K. Jinno (Ed.), Chromatographic Separations Based on Molecular Recognition, Wiley-VCH, New York, 1996, p. 371 (Chapter 7).
[7] V. Schurig, J. Chromatogr. A 965 (2002) 315.
[8] C.C. Hu, C.Y. Liu, Anal. Chim. Acta 332 (1996) 23.
[9] C.Y. Liu, C.C. Hu, C.L. Yang, J. Chromatogr. A 773 (1997) 199.
[10] C.Y. Liu, C.C. Hu, J.L. Chen, K.T. Liu, Anal. Chim. Acta 384 (1999) 51.
[11] C.Y. Liu, J.L. Chen, C.C. Shiue, K.T. Liu, J. Chromatogr. A 862 (1999) 65.
[12] C.Y. Liu, S.H. Yang, M.H. Chau, C.C. Shiue, J. Chromatogr. A 933 (2001) 117.
[13] C.T. Chou, Y.F. Pai, C.C. Lin, T.K. Misra, C.Y. Liu, J. Chromatogr. A 1043 (2004) 255.
[14] L.A. Komarnisky, R.J. Christopherson, T.K. Basu, Nutrition 19 (2003) 54.
[15] R.G. Hendrickson, A. Chang, R.J. Hamilton, Am. J. Ind. Med. 45 (2004) 346.
[16] J. Maukonen, M. Saarela, L. Raaska, J. Ind. Microbiol. Biotechnol. 33 (2006) 45.
[17] E.J. Shelley, D. Ryan, S.R. Johnson, M. Couillard, D. Fitzmaurice, P.D. Nellist, Y. Chen, R.E. Palmer, J.A. Preece, Langmuir 18 (2002) 1791.
[18] D.B. Pedersen, S. Duncan, J. Phys. Chem. A 109 (2005) 11172.
[19] A. Perl, M. Péter, B.J. Ravoo, D.N. Reinhoudt, J. Huskens, Langmuir 22 (2006) 7568.
[20] H. Behbehani, M.A. Al-Qallaf, O.M.E. EL-Dusouqui, Petrol. Sci. Technol. 23 (2005) 219.
[21] K. Korhonen, A.T. Liukkonen, A.W. Ahrens, et al., Int. Arch. Occup. Environ. Health 77 (2004) 451.
[22] H.M. Burbank, M.C. Qian, J. Chromatogr. A 1066 (2005) 149.
[23] Y. Fang, M.C. Qian, J. Chromatogr. A 1080 (2005) 177.
[24] A. Sakamoto, T. Niki, Y.W. Watanabe, Anal. Chem. 78 (2006) 4593.
[25] R. Hua, J. Wang, H. Kong, J. Liu, X. Lu, G. Xu, J. Sep. Sci. 27 (2004) 691.
[26] J.L. Chen, C.Y. Liu, Anal. Chim. Acta 548 (2005) 73–78.
[27] F. Ammar-Khodja, S. Guermouche, M.H. Guermouche, E. Rogalska, M. Rogalski, P. Judeinstein, J.P. Bayle, Chromatographia 57 (2003) 249.